

# A high-precision instrument for mapping of rotational errors in rotary stages

Weihe Xu, Kenneth Lauer, Yong Chu and Evgeny Nazaretski\*

Received 4 June 2014

Accepted 11 July 2014

Photon Sciences, Brookhaven National Laboratory, Upton, NY 11973, USA. \*E-mail: enazaretski@bnl.gov

A rotational stage is a key component of every X-ray instrument capable of providing tomographic or diffraction measurements. To perform accurate three-dimensional reconstructions, runout errors due to imperfect rotation (*e.g.* circle of confusion) must be quantified and corrected. A dedicated instrument capable of full characterization and circle of confusion mapping in rotary stages down to the sub-10 nm level has been developed. A high-stability design, with an array of five capacitive sensors, allows simultaneous measurements of wobble, radial and axial displacements. The developed instrument has been used for characterization of two mechanical stages which are part of an X-ray microscope.

© 2014 International Union of Crystallography

**Keywords:** high-precision instrument; rotational errors; rotary stages.

## 1. Introduction

X-ray microscopy is a powerful tool suitable for studies of the internal structure and composition of various material systems (Ice *et al.*, 2011; Kaulich *et al.*, 2011; Kang *et al.*, 2013). Recent developments of ultra-brilliant synchrotron facilities stimulated development of X-ray imaging techniques and pushed the imaging resolution down to the nanometer level (Yan *et al.*, 2014). In the soft X-ray regime, two-dimensional full-field imaging with better than 10 nm spatial resolution has been demonstrated using a Fresnel zone plate as the focusing optics (Chao *et al.*, 2012). In the hard X-ray regime, Huang *et al.* (2013) reported one-dimensional focusing down to 11 nm using multilayer Laue lenses. By taking a series of two-dimensional X-ray projections at different angles, a three-dimensional image of a sample can be reconstructed revealing its internal structure and composition (Kaulich *et al.*, 2011; Holt *et al.*, 2013; Wu *et al.*, 2012). For ptychography imaging, 16 nm spatial resolution has been reported in three dimensions (Holler *et al.*, 2012, 2014). For all tomographic measurements, particularly *via* scanning X-ray microscopy, rotational errors play a critical role in defining scientific throughput of a microscope unless actively corrected (Holler *et al.*, 2012, 2014). Therefore, characterization of displacements due to wobble, axial and radial runouts in rotary stages prior to the measurements is necessary during development of microscopy systems for three-dimensional nanotomography.

A typical method of characterizing rotary stages includes the attachment of a ball gauge to the center of a stage and monitoring its displacement when rotating by sensors (Noire *et al.*, 2010). Non-contact displacement sensors (capacitive, optical *etc.*) are usually employed for high-precision characterization (Marco, 2010; Kim *et al.*, 2013). Unfortunately, such ball gauge systems do not provide simultaneous measurements of displacement errors due to wobble, radial and axial runout errors. In this work, we present a system capable of comprehensive characterization of all rotational errors during the same measurement. By incorporating five capacitive sensors and a diamond-turned reference cylinder, nanometer-scale rotational errors can be measured. A mechanically stiff yet instru-

mentally flexible design allows the mapping of rotational errors in stages with different form factors and footprints.

## 2. Instrument design

A computer-aided design drawing and a photograph of the instrument are shown in Figs. 1(a) and 1(b). The instrument has a robust yet flexible frame structure to provide stability while allowing characterization of rotary stages with different footprints and form factors. Five Lion Precision CPL 190 capacitive displacement sensors with C5S-2.0 probes were arranged in the middle of the beam as shown in Fig. 1(b). Sensors S1 and S2 measure the displacement of the cylinder in the *X* direction, S3 and S4 in the *Y* direction and S5 in the *Z* direction. The rotary stage under investigation is placed on top of a high-precision Kohzu YM16A-S1 *X*-*Y* manual linear stage. The linear stage provides 25 mm travel in both *X* and *Y* directions and yields 0.5  $\mu\text{m}$  resolution. The manual stage is used to position the rotary stage to be characterized within the working ranges of the capacitive sensors. On top of the rotary stage, there is an assembly of *X* and *Y* linear piezo stages (Attocube ECS3030/NUM) with the diamond-turned reference cylinder finally on top of that. Piezo stages are used for the alignment of the cylinder axis and the rotary stage center of rotation. The reference cylinder is 40 mm tall and 25 mm in diameter. It also has a diamond-turned top surface with a machined pin in the center and is used for the initial optical alignment with a CCD camera (BASLER Ace acA1300-30gc). The surface roughness of the reference cylinder was measured with a Zygo optical surface profiler and yielded peak-to-valley values of  $\pm 11$  nm [see Figs. 1(c) and 1(d)]. Since the diameter of the capacitive C5S-2.0 probe is about 2 mm, the localized roughness is averaged and it provides an RMS noise of approximately  $\pm 2$  nm. The system is largely controlled through a LabVIEW interface. The interface communicates with some hardware directly, and indirectly interfaces with the remainder through the Experimental Physics and Industrial Control System (EPICS) channel access protocol.

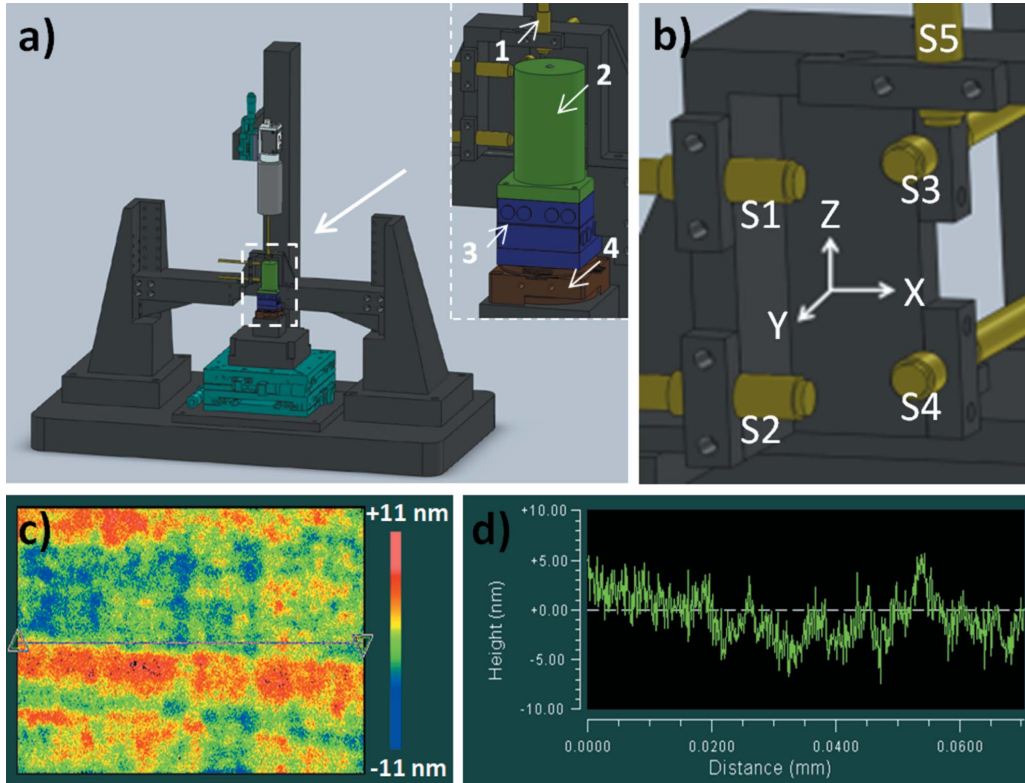


**Figure 1** (a) Schematic view of the instrument. Major components are enumerated: (1) capacitive sensors; (2) high-precision diamond-turned aluminium reference cylinder; (3) X–Y piezo positioner; (4) rotary stage under testing. (b) Arrangement of five Lion Precision CPL 190 capacitive displacement sensors (S1–S5) used to map rotational errors. Surface roughness (c) and line profile (d) of the aluminium reference cylinder acquired with a Zygo white beam interferometer.

### 3. Testing procedures and experimental result

When rotational motion is performed, lateral displacement of a cylinder  $D$  can be expressed as follows,

$$D = D_{\text{runout}} + D_{\text{wobble}} + D_{\text{off-center}}, \quad (1)$$

where  $D_{\text{runout}}$  and  $D_{\text{wobble}}$  are the displacements caused by radial runout and wobble, respectively. Some of the errors are synchronous (repeatable) and some of the errors are asynchronous (random).  $D_{\text{off-center}}$  is the displacement caused by misalignment between the axis of a cylinder and the rotational axis of the rotary stage. Displacements measured by sensors S1–S4 can be written as

$$D_1 = A \cos \alpha + L \sin \theta \cos \beta + R_{13} \cos \omega t, \quad (2)$$

$$D_2 = A \cos \alpha + (L - d_{12}) \sin \theta \cos \beta + R_{24} \cos \omega t, \quad (3)$$

$$D_3 = A \sin \alpha + L \sin \theta \sin \beta + R_{13} \sin \omega t, \quad (4)$$

$$D_4 = A \sin \alpha + (L - d_{12}) \sin \theta \sin \beta + R_{24} \sin \omega t, \quad (5)$$

where  $A$  and  $\alpha$  are the magnitude and phase of the runout,  $\theta$  and  $\beta$  are the magnitude and phase of the wobble.  $L$  is the measured distance from S1 to the top surface of the rotary stage,  $d_{12}$  is the distance between S1 and S2, and  $R_{13}$  and  $R_{24}$  are the distances between the cylinder’s center of rotation in the planes S1–S3 and S2–S4, respectively. By fitting the measured values of  $D_{1-4}$  to  $\sin \omega t$  and  $\cos \omega t$ , values of  $R_{13}$  and  $R_{24}$  can be calculated and subsequently subtracted from  $D_{1-4}$ . Finally, since values of  $L$  and  $d_{12}$  are directly measured, values of  $\theta$  and  $\beta$  can be calculated yielding  $A$  and  $\alpha$ .

Displacements measured by S5 can be written as follows,

$$D_5 = D_{\text{wobble}} + D_{\text{tilt}} + D_{\text{vertical displacement}} \quad (6)$$

$$= R_5 \sin \theta \cos \beta + R_5 \sin \gamma \cos \omega t + D_{\text{vertical displacement}}$$

where  $D_{\text{tilt}}$  is the displacement caused by tilting of the cylinder.  $D_{\text{vertical displacement}}$  is the displacement caused by the vertical motion (axial runout).  $R_5$  is the distance from the measurement point of sensor S5 to the rotation center.  $\gamma$  is the tilting angle of the cylinder. By fitting the measured values of  $D_5$  to  $\cos \omega t$ , values of  $R_5$  can be calculated. Since the values of  $\theta$  and  $\beta$  at each rotational angle have been measured,  $D_{\text{vertical displacement}}$  can then be calculated.

To verify the performance of the developed system, we fully characterized rotational errors of two mechanical rotary stages, referred to here as stage 1 and stage 2. Stage 1 is an Attocube ANR240/RES. It has a small footprint, uses a stick-slip piezoelectric actuator and is encoded from 0 to 320° [shown in Figs. 1(a) and 1(b)]. Stage 2 is a KOHZU RA10A-W. It has a larger form factor and has a rotation range between 0 and 280°. Measurements for each stage were repeated six times and the results are depicted in Fig. 2. For stage 1, radial runout, wobble and axial runout were measured to be  $6 \pm 5 \mu\text{m}$ ,  $200 \pm 150 \mu\text{rad}$  and  $\pm 0.6 \mu\text{m}$ , respectively. For stage 2, the measured values were  $0.4 \pm 0.4 \mu\text{m}$ ,  $6 \pm 6 \mu\text{rad}$  and  $\pm 0.08 \mu\text{m}$ , respectively. Based on the measurements shown in Fig. 2, one can determine that runout and wobble for both stages are highly repeatable. The most prominent example is the 2° periodic error measured for stage 2. Because the majority of rotational errors are reproducible, synchronous deviations from a perfect trajectory can be programmed into tomographic data acquisition software, and the

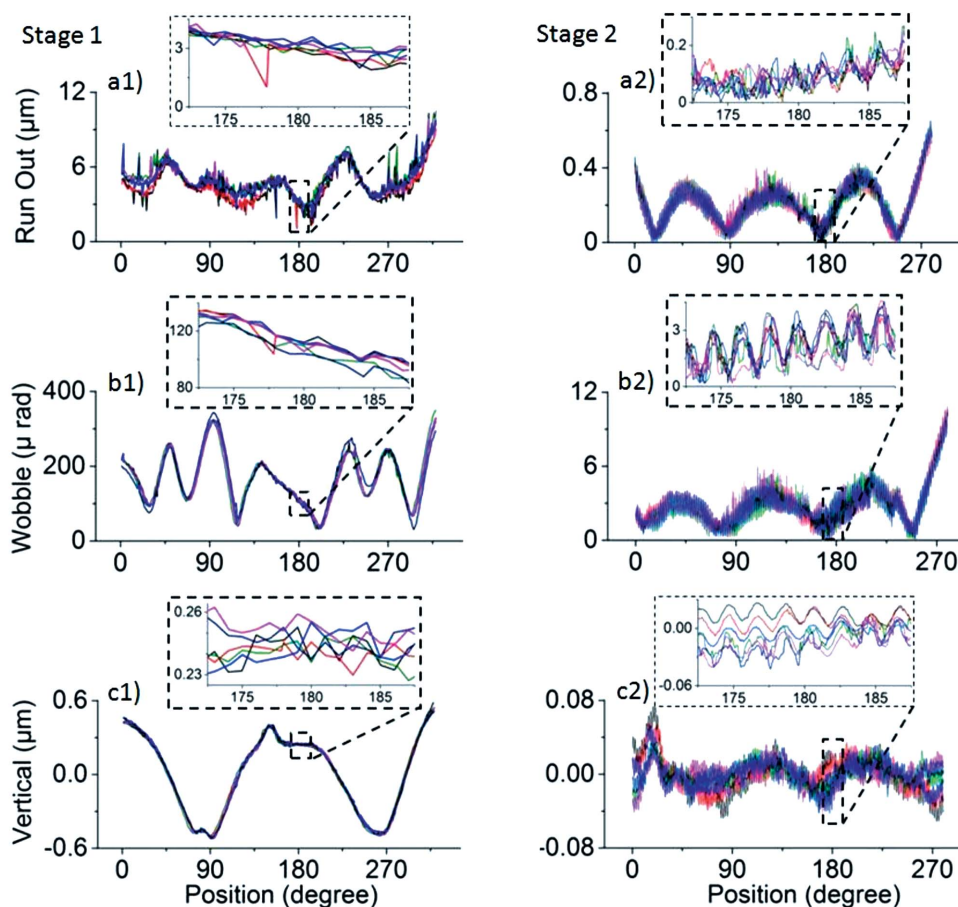


**Figure 2**  
(a1–a2) Radial runout error of stage 1 and stage 2, (b1–b2) wobble of stage 1 and stage 2, (c1–c2) axial runout error of stage 1 and stage 2.

field of view can be adjusted accordingly during measurements of each individual projection. In doing so, the data acquisition time can be reduced yielding a higher throughput for the tomographic system.

#### 4. Conclusion

In this work, we have developed a high-precision instrument suitable for the characterization of rotational stages used in three-dimensional tomographic measurements. The instrument provides simultaneous measurements of both radial and axial runouts and wobble in a rotary stage. Stable structural design, application of five capacitor sensors and a diamond-turned reference cylinder ensure nanometer-level mapping of rotational errors. The developed system was used to characterize two mechanical rotary stages and revealed both synchronous and asynchronous errors.

We acknowledge B. Mullany (BNL) for help with three-dimensional modeling of the microscope and D. Kuhne (BNL) for machining and assembling of mechanical parts. Work at BNL was supported by the US Department of Energy under contract No. DE-AC02-98CH10886.

#### References

- Chao, W., Fischer, P., Tyliczszak, T., Rekawa, S., Anderson, E. & Naulleau, P. (2012). *Opt. Express*, **20**, 9777–9783.
- Holler, M. J., Diaz, A., Guizar-Sicairos, M., Karvinen, P., Färm, E., Härkönen, E., Ritala, M., Menzel, A., Raabe, J. & Bunk, O. (2014). *Sci. Rep.* **4**, 3857.
- Holler, M., Raabe, J., Diaz, A., Guizar-Sicairos, M., Quitmann, C., Menzel, A. & Bunk, O. (2012). *Rev. Sci. Instrum.* **83**, 073703.
- Holt, M., Harder, R., Winarski, R. & Rose, V. (2013). *Annu. Rev. Mater. Res.* **43**, 183–211.
- Huang, X., Yan, H., Nazaretski, E., Conley, R., Bouet, N., Zhou, J., Lauer, K., Li, L., Eom, D., Legnini, D., Harder, R., Robison, I. K. & Chu, Y.-S. (2013). *Rev. Sci. Instrum.* **84**, 035006.
- Ice, G. E., Budai, J. D. & Pang, J. W. L. (2011). *Science*, **334**, 1234–1239.
- Kang, H. C., Yan, H., Chu, Y. S., Lee, S. Y., Kim, J., Nazaretski, E., Kim, C., Seo, O., Noh, D. Y., Macrander, A. T., Stephenson, G. B. & Maser, J. (2013). *Nanoscale*, **5**, 7184–7187.
- Kaulich, B., Thibault, P., Gianoncelli, A. & Kiskinova, M. (2011). *J. Phys. Condens. Matter*, **23**, 083002.
- Kim, J., Lauer, K., Yan, H., Chu, Y. S. & Nazaretski, E. (2013). *Rev. Sci. Instrum.* **84**, 035006.
- Marco, S. (2010). *Evaluation of the Sphere of Confusion of Goniometer Devices and Analysis of the SmarAct Linear Positioners*. Internship report.
- Noire, P., Jonquieres, N., Schlutig, S., Leterme, D. & Roux, T. (2010). *Diamond Light Source Proc.* **1**, 1–4.
- Wu, H. R. *et al.* (2012). *J. Phys. D*, **45**, 242001.
- Yan, H., Conley, R., Bouet, N. & Chu, Y. S. (2014). *J. Phys. D*, **47**, 263001.